

Dependence of spontaneous polarization on stacking sequence in SiC revealed by local Schottky barrier height variations over a partially formed 8H-SiC layer on a 4H-SiC substrate

Kibog Park, Heung Seok Go, Youngeun Jeon, Jonathan P. Pelz, Xuan Zhang et al.

Citation: *Appl. Phys. Lett.* **99**, 252102 (2011); doi: 10.1063/1.3670329

View online: <http://dx.doi.org/10.1063/1.3670329>

View Table of Contents: <http://apl.aip.org/resource/1/APPLAB/v99/i25>

Published by the AIP Publishing LLC.

Additional information on Appl. Phys. Lett.

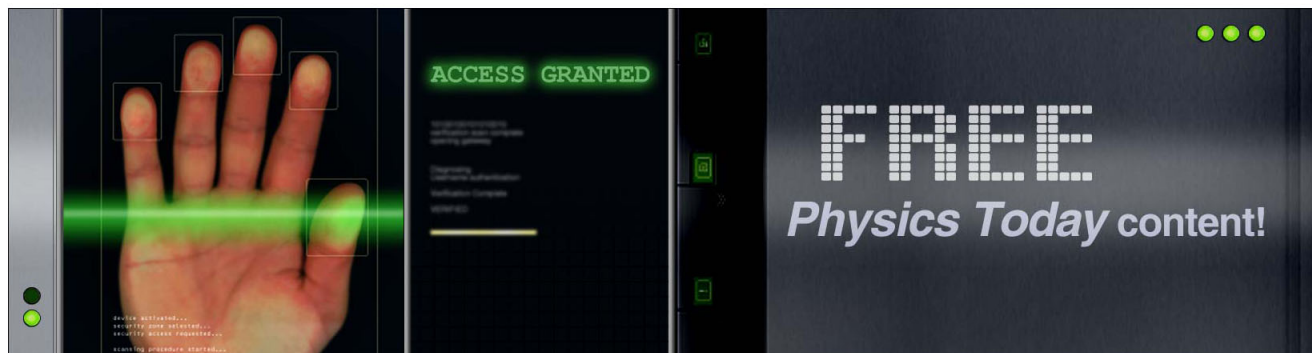
Journal Homepage: <http://apl.aip.org/>

Journal Information: http://apl.aip.org/about/about_the_journal

Top downloads: http://apl.aip.org/features/most_downloaded

Information for Authors: <http://apl.aip.org/authors>

ADVERTISEMENT



Dependence of spontaneous polarization on stacking sequence in SiC revealed by local Schottky barrier height variations over a partially formed 8H-SiC layer on a 4H-SiC substrate

Kibog Park,^{1(a)} Heung Seok Go,¹ Youngeun Jeon,¹ Jonathan P. Pelz,² Xuan Zhang,³ and Marek Skowronski⁴

¹*School of Electrical and Computer Engineering, Ulsan National Institute of Science and Technology, Ulsan 689-798, Korea*

²*Department of Physics, The Ohio State University, Columbus, Ohio 43210, USA*

³*Central Research Institute of Electric Power Industry (CRIEPI), 2-6-1 Nagasaka, Yokosuka, Kanagawa 240-0196, Japan*

⁴*Department of Materials Science and Engineering, Carnegie Mellon University, Pittsburgh, Pennsylvania 15213, USA*

(Received 18 September 2011; accepted 17 November 2011; published online 19 December 2011)

Ballistic electron emission microscopy was used to measure the increase of local Schottky barrier (compared to the surrounding 4H-SiC area) over a partial 8H-SiC layer that is the surface-exposed tail of an 8H stacking fault inclusion extending from 4H substrate. This local increase is believed to be due to polarization charge induced at the interface of partial 8H layer and underlying 4H host, resulting from the spontaneous polarization (SP) difference between SiC regions with different bilayer stacking. This is a direct experimental probe of the dependence of SP in SiC on local stacking sequence by measuring carrier transport. © 2011 American Institute of Physics. [doi:10.1063/1.3670329]

In addition to the many superior physical and chemical properties of SiC that make it a prominent candidate for high-temperature, high-power, and high-frequency electronic devices,¹ SiC also possesses the fundamentally interesting property of *spontaneous polarization* (SP). In particular, the SP in SiC is unique in that it depends strongly on *structural polytype*. SiC is known to crystallize in many different polytypes (more than 200) that are based on the stacking sequence of Si-C basal plane bilayers.² Due to crystal symmetry, only the polytypes with so called “hexagonal turns” in the Si-C bilayer stacking (including the 4H-, 6H-, 8H-, and 15R-SiC polytypes) show SP, while 3C-SiC (with cubic zinc-blende structure) does not.^{3,4} Qteish *et al.* have shown theoretically that electric dipole layer (the basic unit of SP) forms at a hexagonal turn due to electron redistribution and ionic relaxation, and that the SP varies almost linearly with hexagonality (defined as the fraction of hexagonal stackings out of all stackings).³ In this letter, we present direct measurements made with ultra-high vacuum (UHV) ballistic electron emission microscopy (BEEM) (Ref. 5) of the increase of the local Schottky barrier height (SBH) over a thin SiC slab which is the *surface-exposed portion* of an 8H-SiC stacking fault (SF) inclusion originating from the bulk, as compared with the SBH measured over the surrounding 4H area. We believe that the increase of the local SBH over this thin (<2 nm thick) partial 8H layer results from the interface-bound polarization charge due to the SP difference between the partial 8H layer and the underlying 4H-SiC substrate.

It has been reported recently^{6,7} that planar SFs can form during the chemical vapor deposition (CVD) growth of epilayers on off-cut 4H-SiC substrates, with the SFs comprised

of one complete unit of 8H stacking, embedded in the 4H-SiC host crystal. These SF-induced inclusions nucleate at the initial stage of CVD growth and extend through the epilayer. This particular inclusion is similar to the other SF inclusions formed under different growth/processing conditions.^{8–12} The sample used in this study is a 4H-SiC CVD epilayer grown on an n-type 4H-SiC substrate 8° miscut from (0001) towards the (11 $\bar{2}$ 0) orientation. According to our *C-V* measurements, the epilayer doping is $\sim 2 \times 10^{14} \text{ cm}^{-3}$ (n-type). The 8H stacking of the SF inclusions on this sample was confirmed by high-resolution TEM images. The as-grown sample was first degreased (using ultrasonic trichloroethylene, acetone, and methanol for 10 min each), then oxidized in ultra-violet ozone, followed by a final HF (49%) dip and methanol rinse. The sample was then mounted on a sample block and introduced into a UHV preparation chamber, out-gassed overnight at $\sim 200^\circ \text{C}$, then a Pt film with $\sim 5 \text{ nm}$ thickness was evaporated onto the sample surface through a shadow mask to form an array of $\sim 0.5 \text{ mm}$ diameter contacts. The sample was then transferred without breaking vacuum into the attached UHV scanning tunneling microscopy (STM) chamber with BEEM measurement capability.

Figure 1(a) shows a typical large-scale STM topographic image over the Pt overlayer which reveals the morphology of the underlying SiC substrate. 8H inclusions in this sample are found to produce a characteristic asymmetric V-shaped deep groove structure near the “opening” of an inclusion at the surface where the plane of the inclusion intersects the sample surface (the inclusion opening actually indicates the bottom of the groove). We know that the SF inclusions with *complete* 8H stacking terminate at the bottom of the grooves from the BEEM measurements discussed below. Figure 1(b) shows the surface profile measured along

^{a)} Electronic mail: kibogpark@unist.ac.kr. Tel.: +82522172111.

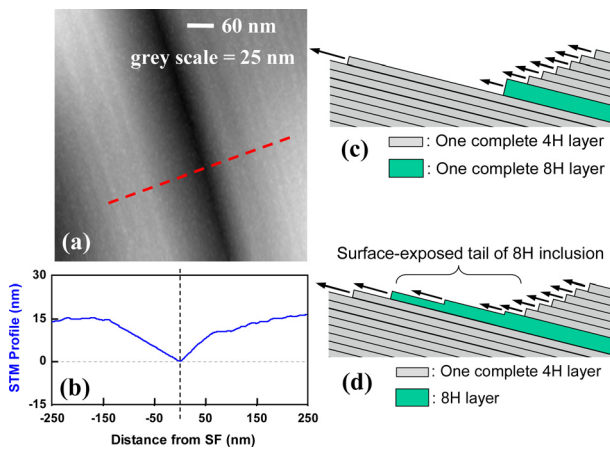


FIG. 1. (Color online) (a) STM morphology over the Pt overlayer revealing the surface structure of the underlying SiC substrate near the opening of 8H SF inclusion and (b) its cross-sectional profile along the path (dotted line) going across the inclusion opening perpendicularly. Schematic diagrams illustrating two possible ways that the 8H inclusion terminates in the groove: (c) abrupt termination with a large step of a complete 8H unit and (d) gradual termination with a series of smaller steps, leaving a surface-exposed “tail” of the 8H inclusion.

the dashed line in Figure 1(a), revealing that both sides of the groove appear to be quite flat. In particular, the flat portion on the left side of the groove extends almost up to ~ 135 nm away from the opening and is found to be almost parallel to the basal plane of the 4H substrate. Since the sample cleaning procedure did not significantly alter the sample morphology, it is believed that this deep groove structure is formed during epilayer growth. While the detailed formation mechanism of the groove structure during epilayer growth is not yet fully understood, one possible explanation is the following: The growth of the epilayer during CVD occurs through the motion of steps. If the growth of some of the steps that bound SiC bilayers in the 8H inclusion is slower than the growth of the steps that bound the 4H-SiC host material, then the advance of the edges of 4H layers residing over the inclusion (which have step edges on the right side of the groove in Figure 1) would be retarded compared with the step edges of the 4H layers underneath the inclusion (which have steps on the left side of the groove). This difference in step velocity would eventually induce the V-shaped groove structure. Figures 1(c) and 1(d) illustrate two possible ways that the 8H inclusion could terminate in the groove. In Figure 1(c), it is assumed to terminate abruptly with a large step that is a full 2 nm thickness of a complete 8H unit, while in Figure 1(d), it is assumed to terminate with a series of smaller steps, leaving a surface-exposed “tail” of the 8H inclusion extending over a large distance. The BEEM measurements discussed below indicate that the extended termination shown in Figure 1(d) is the correct structure. Similar surface corrugation was found over the 3C-inclusions nucleating during SiC epitaxy.¹³ In this case, the thin slab of the 3C-polytype was also exposed on the down-step side of the groove.

Once an 8H inclusion was located on the sample surface, we measured the local BEEM spectra on and away from the inclusion opening. Figure 2 shows two BEEM I_c-V_T curves (each an average of >100 individual curves at a

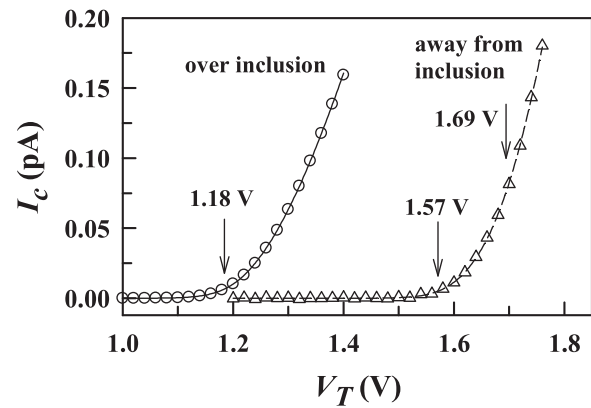


FIG. 2. Typical BEEM spectra (I_c-V_T curves) averaged over ~ 100 individual I_c-V_T curves on an 8H inclusion (open circle) and on the surrounding 4H-SiC far away from it (open triangle). The arrows indicate SBHs determined by fitting the measured data to Bell-Kaiser model. The SB over the 8H inclusion was measured to be ~ 0.39 eV lower than the surrounding 4H substrate, representing the QW energy depth in the inclusion being lower than 4H conduction band minimum by the same amount.

particular location) measured directly over the inclusion opening (left curve) and at a location more than 150 nm away over the surrounding 4H-SiC (right curve). Over the 4H-SiC substrate, the 1.57 eV SBH and characteristic double threshold are essentially the same as measured previously over other 4H-SiC substrates.^{14,15} In contrast, over the 8H inclusion, the SBH was measured to be 0.39 ± 0.01 eV lower, indicating that 8H inclusions embedded in 4H-SiC behave as *electron quantum wells* (QWs), similar to the behavior reported for single- and double-SF 3C inclusions embedded in 4H-SiC.^{10,12}

In addition to confirming the QW behavior of these 8H inclusions, we also observed that the local SBH measured just to the left of the inclusion opening was *substantially higher* than that measured just to the right of the inclusion opening or on areas of the 4H-SiC substrate far from the opening. The square data points in Figure 3(a) show the measured SBH as a function of distance from the opening, where we observe an increased SBH extending a distance of ~ 100 nm on the left side. We note that when the STM tip is within ~ 10 nm of the inclusion opening, the measured SBH is much lower due to the QW nature of the 8H inclusion (see Figure 2) and is not included in Figure 3(a). If the 8H inclusion terminated abruptly at the surface as postulated in Figure 1(c), then both sides of the opening would have a normal Pt/4H-SiC interface and so should have the same SBH. However, since the SBH is actually higher just to the left of the opening, we conclude that a partial layer of the 8H inclusion (with different bilayer stacking than the 4H host) extends out on the left side of the groove, forming a surface-exposed 8H tail as illustrated in Figure 1(d).

We can understand the larger SBH over the 8H tail in a natural way since the SP in 8H-SiC is expected to be smaller than in 4H-SiC,³ resulting in a net “polarization charge” at the 4H/8H interface, which together with the image charge in the metal film will produce a strong electric field across the surface-exposed 8H tail. This will increase the resulting SBH at the metal/8H (partial) interface, as illustrated in Figure 3(b). This proposal is analogous to that proposed by Yu et al.¹⁶ for a GaN/Al_xGa_{1-x}N/GaN/metal structure.

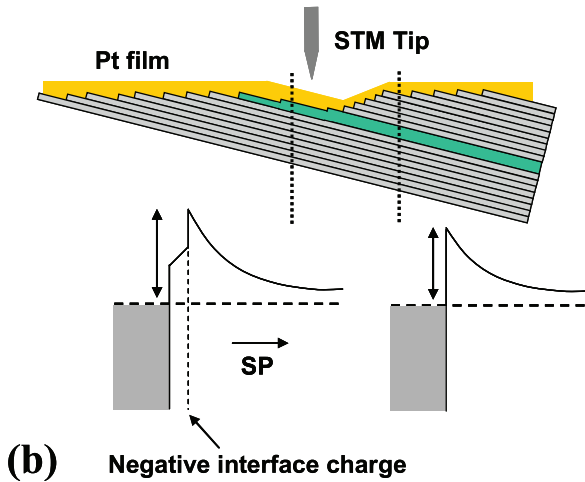
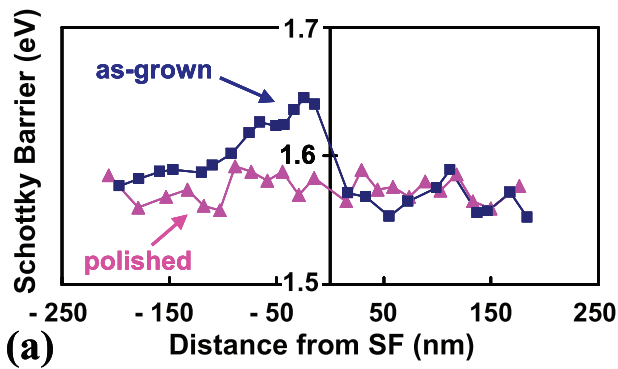


FIG. 3. (Color online) (a) Profile of local SBH near the opening of 8H SF inclusion on the sample surface for both as-grown (square) and surface-polished (triangle) samples and (b) schematics of possible step structures near 8H inclusion opening and energy band diagrams for Pt contact on normal 4H substrate (right) and thin partially formed 8H layer (left) sitting on top of 4H substrate. The negative interface-bound polarization charge due to the SP difference of the partial 8H layer and 4H substrate causes the increase of local SB.

To test this assertion, we chemi-mechanically polished another piece of sample cut from the same wafer to remove the surface groove structure (along with any surface-exposed 8H tail), used BEEM to locate the (polished) inclusion opening (visible as a line of low SBH), and then measured the SBH as a function of distance away from the opening. These measurements are shown as the triangle data points in Figure 3(a). We see that the asymmetry of the SBH on either side of the opening has been removed by the polishing, giving strong support to the proposal that the asymmetry observed on the un-polished sample is due to a surface-exposed 8H tail. As seen in Figure 3(a), on the un-polished sample, the SBH on the left side of the inclusion opening decreases gradually to the value on the surrounding 4H-SiC area as the tip is moved ~ 100 – 150 nm away from the opening. If the inclusion tail on that side had a uniform thickness, the local SBH would be expected to increase abruptly just to the left of the inclusion opening and remain uniform until the edge of the inclusion tail, where it would abruptly return to the “normal” value measured on the rest of the sample. Hence, the observed gradual decrease of SBH seems to indicate that the inclusion tail is not uniform in thickness, rather becomes progressively thinner away from the opening. Further support for this comes from atomic force microscopy (AFM) measurements we made on

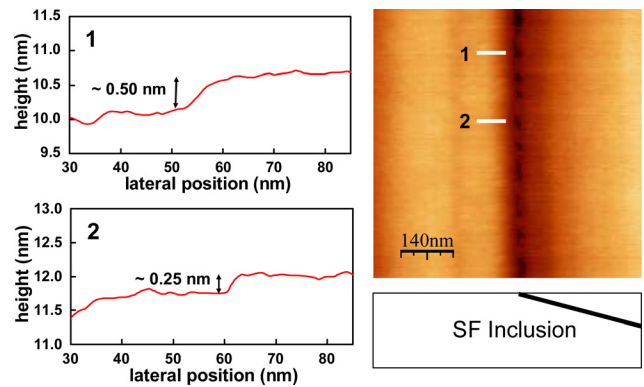


FIG. 4. (Color online) AFM image (right) and height profiles (left) taken on regions of a bare surface (no Pt film) around 8H inclusion opening. In the height profiles, steps with heights of a certain multiple of Si-C bilayer (stacking unit) are visible clearly, indicating random step structure on the area where the tail of 8H SF inclusion originating from the bulk is exposed on the sample surface.

regions of a bare surface (not covered by a Pt film) around the inclusion opening, shown in Figure 4. These AFM measurements indeed show that the inclusion tail appears to have step structure where its thickness decreases by a certain multiple of the Si-C bilayer (stacking unit) across each step. For the particular inclusion shown in Figure 4, the steps along the two profile lines indicated are measured to have a height of either ~ 0.25 nm (one bilayer) or ~ 0.5 nm (two bilayer). These AFM-measurements are exactly consistent with the proposed structure of the surface-exposed 8H tail illustrated in Figure 1(d).

We note that these steps appear at different distances from the inclusion opening as one moves parallel to the opening, and that when the surface is covered with Pt the steps cannot be directly distinguished in the STM images. Hence, it is not possible to measure the local thickness of the 8H-tail at positions where the SBH is measured with BEEM. Hence, we cannot use the locally measured SBH to quantify the SP in the 8H tail. Accordingly we just point out that our measured BEEM-threshold profile and AFM height profiles strongly support the proposal that the partly grown inclusion tail with step structures exists on the left side of the observed groove structure near the 8H inclusion opening on surface.

In summary, we report (1) The 8H inclusions in 4H-SiC behave as electron QWs (with a QW energy ~ 0.39 eV below the 4H-SiC conduction band minimum). (2) The local SBH is asymmetrically higher on one side of the inclusion opening, giving strong support to the proposal that a surface-exposed partial 8H layer extends for ~ 100 – 150 nm away from the opening. (3) The local increase in the SBH is likely due to the interface-bound polarization charge induced by the difference of SP between the partial 8H layer and the 4H substrate. This last observation is an experimental demonstration of directly probing the dependence of SP in SiC on local stacking sequence by measuring carrier transport.

The authors acknowledge M. A. Capano at Purdue University for supplying the SiC samples. The work at the Ohio State University was supported by National Science Foundation Grants DMR-0505165 and DMR-0805237, the work at Carnegie Mellon University was supported by Office of Naval Research grant, N00014-08-1-0338, and the work at Ulsan

National Institute of Science and Technology was supported by National Nuclear R&D Program through the National Research Foundation funded by the Ministry of Education, Science, and Technology in Korea (2011-0006387), by the Korea Research Council of Fundamental Science and Technology through Basic Research Project managed by the Korea Research Institute of Standards and Science, and also by the year of 2009-2010 Research Fund of Ulsan National Institute of Science and Technology (1.090006).

¹*Diamond, SiC, and Nitride Wide Bandgap Semiconductors*, edited by C. H. Carter, Jr., G. Gildenblat, S. Nakamura, R. J. Neimnich, (Materials Research Society, Pittsburgh, 1994).

²A. P. Verma and P. Krishna, *Polymorphism and Polytypism in Crystals* (Wiley, New York, 1966).

³A. Qteish, V. Heine, and R. J. Needs, *Phys. Rev. B* **45**, 6534 (1992).

⁴S. Bai, R. P. Devaty, W. J. Choyke, U. Kaiser, G. Wagner, and M. F. Mac-Millan, *Appl. Phys. Lett.* **83**, 3171 (2003).

⁵W. J. Kaiser and L. D. Bell, *Phys. Rev. Lett.* **60**, 1406 (1988); L. D. Bell and W. J. Kaiser, *Phys. Rev. Lett.* **61**, 2368 (1988).

⁶S. Izumi, H. Tsuchida, T. Tawara, I. Kamata, and T. Tawara, *Appl. Phys. Lett.* **86**, 202108 (2005).

⁷H. Fujiwara, T. Kimoto, T. Tojo, and H. Matsunami, *Appl. Phys. Lett.* **87**, 051912 (2005).

⁸J. P. Bergman, H. Lendenmann, P. A. Nilsson, U. Lindefelt, and P. Skytt, *Mater. Sci. Forum* **353–356**, 299 (2001).

⁹K.-B. Park, Y. Ding, J. P. Pelz, M. K. Mikhov, Y. Wang, and B. J. Skromme, *Appl. Phys. Lett.* **86**, 222109 (2005).

¹⁰K.-B. Park, J. P. Pelz, J. Grim, and M. Skowronski, *Appl. Phys. Lett.* **87**, 232103 (2005).

¹¹R. S. Okojie, M. Zhang, P. Pirouz, S. Tumakha, G. Jessen, and L. J. Brillson, *Appl. Phys. Lett.* **79**, 3056 (2001).

¹²Y. Ding, K.-B. Park, J. P. Pelz, K. C. Palle, M. K. Mikhov, B. J. Skromme, H. Meidia, and S. Mahajan, *Phys. Rev. B* **69**, 041305(R) (2004).

¹³A. O. Konstantinov, C. Hallin, B. Pecz, O. Kordin, E. Janzen, *J. Cryst. Growth* **178**, 495 (1997).

¹⁴B. Kaczer, H.-J. Im, J. P. Pelz, J. Chen, and W. J. Choyke, *Phys. Rev. B* **57**, 4027 (1998).

¹⁵H.-J. Im, B. Kaczer, J. P. Pelz, S. Limpijumnon, W. R. L. Lambrecht, and W. J. Choyke, *J. Electron. Mater.* **27**, 345 (1998).

¹⁶E. T. Yu, X. Z. Dang, L. S. Yu, D. Qiao, P. M. Asbeck, S. S. Lau, G. J. Sullivan, K. S. Boutros, and J. M. Redwing, *Appl. Phys. Lett.* **73**, 1880 (1988)